Fault and Stress Analysis:
user's manual for the FSA software
- - -
Preliminary and incomplete,
yet probably already useful draft
- - -
Version 0.4

Bernard Célérier

2020-06-15

Contents

List of Tables

List of Figures

Chapter 1

General Conventions

2017-05-15

1.1 Introduction

This chapter lays out general definitions and conventions that are useful for the following chapters and that were introduced in previous work (*Célérier*, 1988; *Tajima and Célérier*, 1989; *Célérier*, 1995; *Célérier and Séranne*, 2001; *Burg et al.*, 2005; *Célérier*, 2010).

1.2 Notations

We use a super script convention where the matrix representing a frame or operator F in the reference frame H is written $\mathbf{F^H}$. In the case F is a frame, $F = (\vec{f_1}, \vec{f_2}, \vec{f_3})$, the jth column of $\mathbf{F^H}$ is made of the coordinates of $\vec{f_j}$ in the H frame.

1.3 Parameters

A comprehensive list of all parameters used in this manual is given in Table 1.1.

1.4 Geographical frame

A right handed geographical frame, G, is built with the unit vectors $\vec{g_1}, \vec{g_2}, \vec{g_3}$ pointing north, east and down respectively: $G = (\vec{g_1}, \vec{g_2}, \vec{g_3})$ (*Tajima and Célérier*, 1989; *Célérier*, 2008, 2010).

1.5 Revisions of this chapter

|2017-05-15 |

Table 1.1: Parameters used in this document

Symbol	Comments
	Geographical frame
$G = (\vec{g_1}, \vec{g_2}, \vec{g_3})$	Geographical right-handed frame: $\vec{g_1}, \vec{g_2}, \vec{g_3}$ are unit vectors pointing north, east and down, respectively.
	Fault and slip data
$N = (\vec{n_1}, \vec{n_2}, \vec{n_3})$	Fault plane frame: $\vec{n_1}, \vec{n_2}, \vec{n_3}$ are unit vectors. $\vec{n_1}, \vec{n_2}$ are within the plane and pointing along the strike and dip directions, and $\vec{n_3}$ is the downward pointing normal to the plane.
$E = (\vec{e_1}, \vec{e_2}, \vec{e_3})$	Fault plane and slip frame: $\vec{e_1}, \vec{e_2}, \vec{e_3}$ are unit vectors. $\vec{e_1}, \vec{e_2}$ are within the plane; $\vec{e_1}$ is along the slip direction and $\vec{e_3}$ is the downward pointing normal to the plane.
α	Strike
δ	Dip
λ	Rake
	Stress tensor
$\widehat{\Sigma}$	Full stress tensor
$\widehat{\Sigma_r}$	Reduced stress tensor
$\widehat{I}$	Identity tensor
$S = (\vec{s_1}, \vec{s_2}, \vec{s_3})$	Principal stress directions (right-handed frame)
θ, φ, ψ	Euler's angles used to define S (*Célérier*, 1988)
$\sigma_1 \geqslant \sigma_2 \geqslant \sigma_3$	Principal stress magnitudes (positive compression)
$r_0 = \frac{\sigma_1 - \sigma_2}{\sigma_1 - \sigma_3}$	Stress tensor aspect ratio
$s_0 = \frac{\sigma_1 - \sigma_3}{\sigma_1}$	Normalized stress difference (*Célérier*, 1988; *Tajima and Célérier*, 1989)
$\mathbf{\Sigma^S}$	Matrix of $\widehat{\Sigma}$ in S
$\mathbf{\Sigma_r^S}$	Matrix of $\widehat{\Sigma_r}$ in S

Chapter 2

Fault and slip data

2017-05-15

2.1 Introduction

This chapter introduces two reference frames linked to fault and slip data and then discusses the three major ways of recording the orientation of fault and slip data that can be handled by FSA.

2.2 Fault and slip frames

It is convenient to define two orthogonal frames of unit vectors (Fig. 2.1): one, N, is attached to the fault plane only (*Tajima and Célérier*, 1989; *Célérier*, 1995; *Célérier and Séranne*, 2001; *Célérier*, 2010), and the other, E, to the fault plane with an associated slip direction (*McKenzie*, 1969; *Célérier*, 1988; *Tajima and Célérier*, 1989; *Célérier*, 2010; *Célérier et al.*, 2012).

The first orthogonal frame of unit vectors, $N = (\vec{n_1}, \vec{n_2}, \vec{n_3})$, is attached to the fault plane (Fig. 2.1):

- $\vec{n_1}$ is along the strike direction and so that the plane dips to its right,

- $\vec{n_2}$ is within the plane and along the dip direction, and

- $\vec{n_3}$ is the downward pointing normal to the plane, so that N is right-handed.

The second orthogonal frame of unit vectors, $E = (\vec{e_1}, \vec{e_2}, \vec{e_3})$, is attached to the fault plane and slip direction (Fig. 2.1):

- $\vec{e_1}$ is along the slip direction of the hanging wall with respect to the footwall,
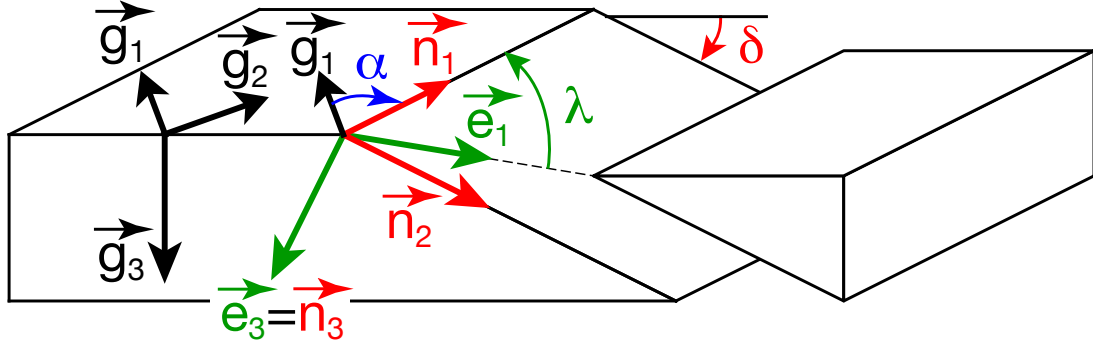
Figure 2.1: Fault and slip orientation: strike, α, dip δ, and rake λ. Geographical frame $G = (\vec{g_1}, \vec{g_2}, \vec{g_3})$, fault plane frame $N = (\vec{n_1}, \vec{n_2}, \vec{n_3})$, and fault and slip frame $E = (\vec{e_1}, \vec{e_2}, \vec{e_3})$.

- $\vec{e_3}$ is the downward pointing normal to the plane, and

- $\vec{e_2}$ is normal to both $\vec{e_1}$ and $\vec{e_3}$ and chosen so that E is right-handed

2.3 Strike, dip, rake with Aki & Richards' convention

This representation is extensively used in seismological databases and corresponds to the internal representation within FSA. It is concise, fully numerical, unambiguous, and clearly and precisely defined in *Aki and Richards* (1980) p.106 or *Aki and Richards* (2002) p. 101. Three angles are recorded (Fig. 2.1):

- strike, α, is in [0,360] and is the azimuth of the horizontal direction chosen so that the plane dips to the right, i.e. $\vec{n_1}$,

- dip, δ, is the plunge of $\vec{n_2}$ in [0,90], and

- defining the slip direction as that of the hanging wall with respect to the footwall, rake, λ, is the angle between the strike, $\vec{n_1}$, and the slip direction, $\vec{e_1}$, measured contra-clockwise from above.

Example: 30 60 -20

The three angles, α, δ, and $-\lambda$ are equivalent to *Euler*'s (1767) angles (Fig. 2.2) :

- a first rotation of angle α around $\vec{g_3}$ transforms the geographical frame, G, into the frame $U = (\vec{u_1}, \vec{u_2}, \vec{u_3})$,

- a second rotation of angle δ around $\vec{u_1}$ transforms U into N, and
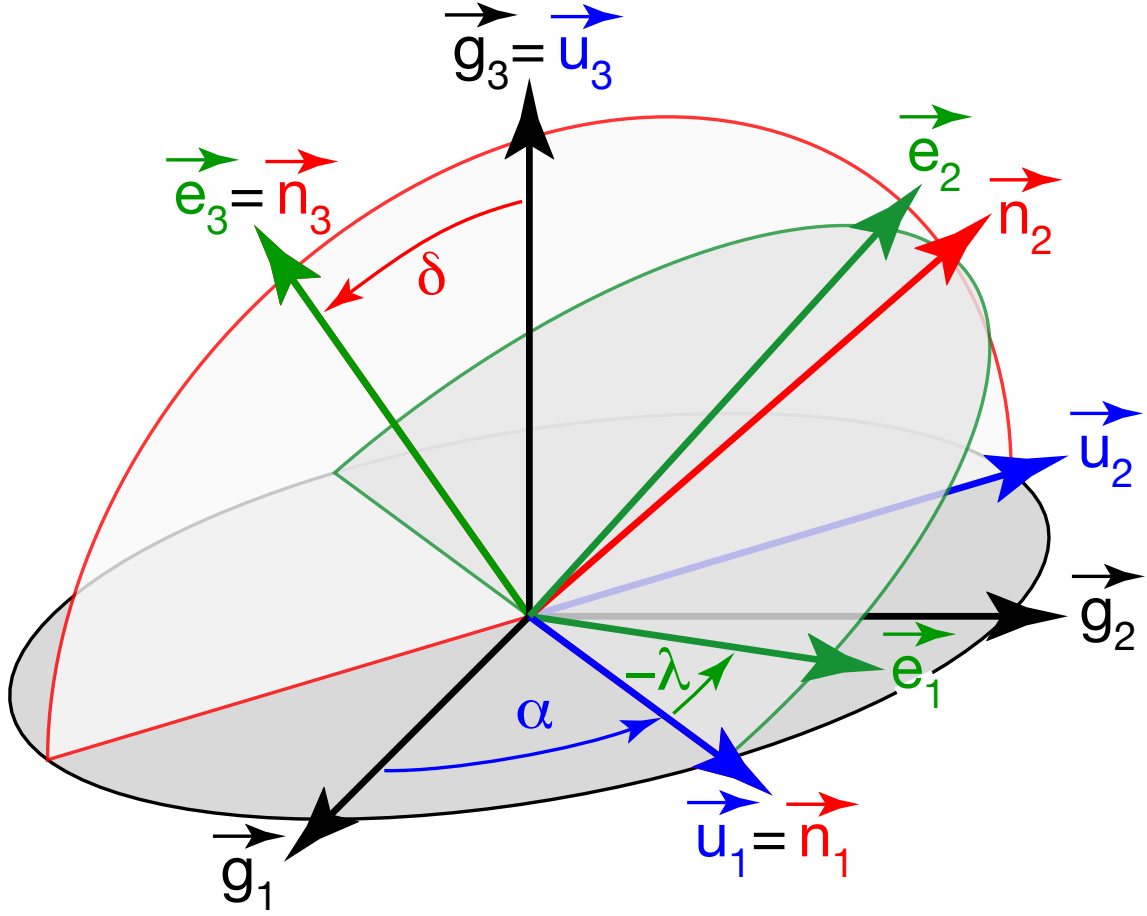
Figure 2.2: *Euler*'s (1767) angles transforming the geographical frame $G = (\vec{g_1}, \vec{g_2}, \vec{g_3})$ into the fault and slip frame $E = (\vec{e_1}, \vec{e_2}, \vec{e_3})$ through 3 successive rotations of angles α, δ, and $-\lambda$. The intermediate stages are $U = (\vec{u_1}, \vec{u_2}, \vec{u_3})$ and $N = (\vec{n_1}, \vec{n_2}, \vec{n_3})$.

- a third rotation of angle $-\lambda$ around $\vec{n_3}$ transforms N into E.

The relationship between rake, λ, taken in [-180,180] and fault movement type is given in Table 2.1 .

2.4   Field measurements: strike, dip, pitch

This is one of two representations used for recording field structural measurements in the former Structural Geology Lab of Montpellier and implemented in the original FAILLE program (*Etchecopar et al.*, 1981; *Etchecopar*, 1984). It is appropriate for high dip planes where pitch measurements are accurate, but must be replaced by the strike, dip, trend representation for low dip planes where pitch measurements become inaccurate. Contrary to many other formats, it does not require any correction on strike angle measurements,

Table 2.1: Rake intervals versus fault movement types

	Sinistral	Dextral
Reverse	[0 , 90]	[90, 180]
Normal	[-90, 0]	[-180, -90]

but take them as directly read on the compass. This eliminates many sources of error, but requires to record two quadrants orientations. Six parameters, 3 numbers and 3 words, are recorded:

- Strike is in [0,360] and is one of the two possible azimuths of the horizontal direction

- Dip angle is in [0,90]

- Dip direction is indicated by a quadrant: North, South, East or West

- Pitch is the angle in [0,90] between one of the strike direction and the slip direction; this strike direction is chosen among the two opposite possibilities so that the pitch angle remains acute.

- Pitch quadrant indicates the quadrant where lies the strike direction chosen to measure pitch. It is recorded as North, South, East or West

- Movement type: Normal, Reverse, Dextral, Sinistral

Example (same as previous example):
30 60 East, pitch 20 North, Sinistral

2.5   Field measurements: strike, dip, trend

This is the other of two representations used for recording field structural measurements in the former Structural Geology Lab of Montpellier and implemented in the original FAILLE program (*Etchecopar et al.*, 1981; *Etchecopar*, 1984). It is appropriate for low dip planes where trend measurements are accurate, but must be replaced by the strike, dip, pitch representation for high dip planes where trend measurements become inaccurate. It does not require any correction on strike angle measurements, but take them as directly read on the compass. This eliminates many sources of error, but requires to record one quadrant orientation. Five parameters, 3 numbers and 2 words, are recorded:

- Strike is in [0,360] and is one of the two possible azimuths of the horizontal direction.

- Dip angle is in [0,90]

- Dip direction is indicated by a quadrant: North, South, East or West

- Trend is one of the two azimuths in [0,360] of the vertical plane that contains the slip direction.

- Movement type: Normal, Reverse, Dextral, Sinistral

Example (same as previous examples):
30 60 East, trend 40, Sinistral

2.6 Field measurements: dip direction, dip, trend, plunge

This representation is more convenient with certain types of compass that directly indicate dip direction or can measure plunge more easily than pitch. Five parameters, 4 numbers and 1 word, are recorded:

- Dip direction is in [0,360].

- Dip angle is in [0,90]

- Slip direction trend in [0,360]

- Slip direction plunge in [0,90]

- Movement type: Normal, Reverse, Dextral, Sinistral

Example (same as previous examples):
120 60, 40 17, Sinistral

2.7 Revisions of this chapter

|2016-10-04 |2017-05-15 |

Chapter 3

Stress data

2016-05-11

3.1 Introduction

This chapter discusses how stress tensor data are handled by FSA.

3.2 Stress tensor

We define three unit vectors, $\vec{s_1}$, $\vec{s_2}$, and $\vec{s_3}$, along the eigenvectors of the stress tensor, $\widehat{\Sigma}$, i.e., along the principal stress directions,

- so that they correspond to the eigenvalues, i.e., the principal stress magnitudes, ordered as $\sigma_1 \geqslant \sigma_2 \geqslant \sigma_3$, with the rock mechanics convention that compression is positive, and

- so that the frame $S = (\vec{s_1}, \vec{s_2}, \vec{s_3})$ is right-handed.

The full stress tensor, $\widehat{\Sigma}$, can be decomposed as:

$$\widehat{\Sigma} = (\sigma_1 - \sigma_3) \cdot \widehat{\Sigma_r} + \sigma_3 \cdot \widehat{I} \tag{3.1}$$

where $\widehat{\Sigma_r}$ is the reduced stress tensor and $\widehat{I}$ the identity tensor. $\widehat{\Sigma}$ and $\widehat{\Sigma_r}$ share the same eigenvectors, $\vec{s_1}$, $\vec{s_2}$, and $\vec{s_3}$, but have different eigenvalues: in the S frame, the full stress tensor, $\widehat{\Sigma}$, is represented by the matrix $\mathbf{\Sigma^S}$

$$\mathbf{\Sigma^S} = \begin{bmatrix} \sigma_1 & 0 & 0 \\ 0 & \sigma_2 & 0 \\ 0 & 0 & \sigma_3 \end{bmatrix} \tag{3.2}$$

whereas the reduced stress tensor, $\widehat{\Sigma_r}$, is represented by $\mathbf{\Sigma_r^S}$

$$\mathbf{\Sigma_r^S} = \begin{bmatrix} 1 & 0 & 0 \\ 0 & 1 - r_0 & 0 \\ 0 & 0 & 0 \end{bmatrix} \tag{3.3}$$

where r_0 is the stress tensor aspect ratio

$$r_0 = \frac{\sigma_1 - \sigma_2}{\sigma_1 - \sigma_3} \tag{3.4}$$

The full stress tensor has 6 independent parameters:

- 3 principal stress magnitudes, $\sigma_1, \sigma_2, \sigma_3$, and

- 3 parameters that define the orientation of the principal stress directions, i.e., of the S frame.

The reduced stress tensor has only 4 independent parameters:

- the stress tensor aspect ratio, r_0, and

- 3 parameters that define the orientation of the principal stress directions, i.e., of the S frame.

Slip inversion constrains the reduced stress tensor only, but frictional analysis requires an extra parameter, s_0 (*Célérier*, 1988; *Tajima and Célérier*, 1989; *Burg et al.*, 2005; *Célérier et al.*, 2012):

$$s_0 = \frac{\sigma_1 - \sigma_3}{\sigma_1} \tag{3.5}$$

With this parameter, equation (3.1) can be recast as:

$$\widehat{\Sigma} = \sigma_1 \cdot s_0 \cdot \widehat{\Sigma_r} + \sigma_3 \cdot \widehat{I} \tag{3.6}$$

3.3 Principal stress directions parameters

The reduced stress tensor is defined by r_0 and the principal stress directions, i.e., the S frame. These directions can be defined either as 3 Euler's angles or as 6 trend and plunge angles.

3.3.1 Euler's angles

Euler's (1767) angles transform a right handed orthonormal frame into another right handed orthonormal frame through 3 successive rotations of angles θ, φ, and ψ. They can thus be used to parametrize the transformation of geographical frame, G, into S, following *Célérier* (1988) (Fig. 3.1). One of the advantages of this representation is that

it relies on three independent parameters. It is always possible to choose the S frame with two downgoing vectors, but not three, because of the constraint that it be right handed. Choosing downgoing $\vec{s_1}$ and $\vec{s_3}$ restrains the angles to:

- $\theta \in [0\,°, 360\,°]$

- $\varphi \in [0\,°, 90\,°]$

- $\psi \in \,] -90\,°, +90\,°]$
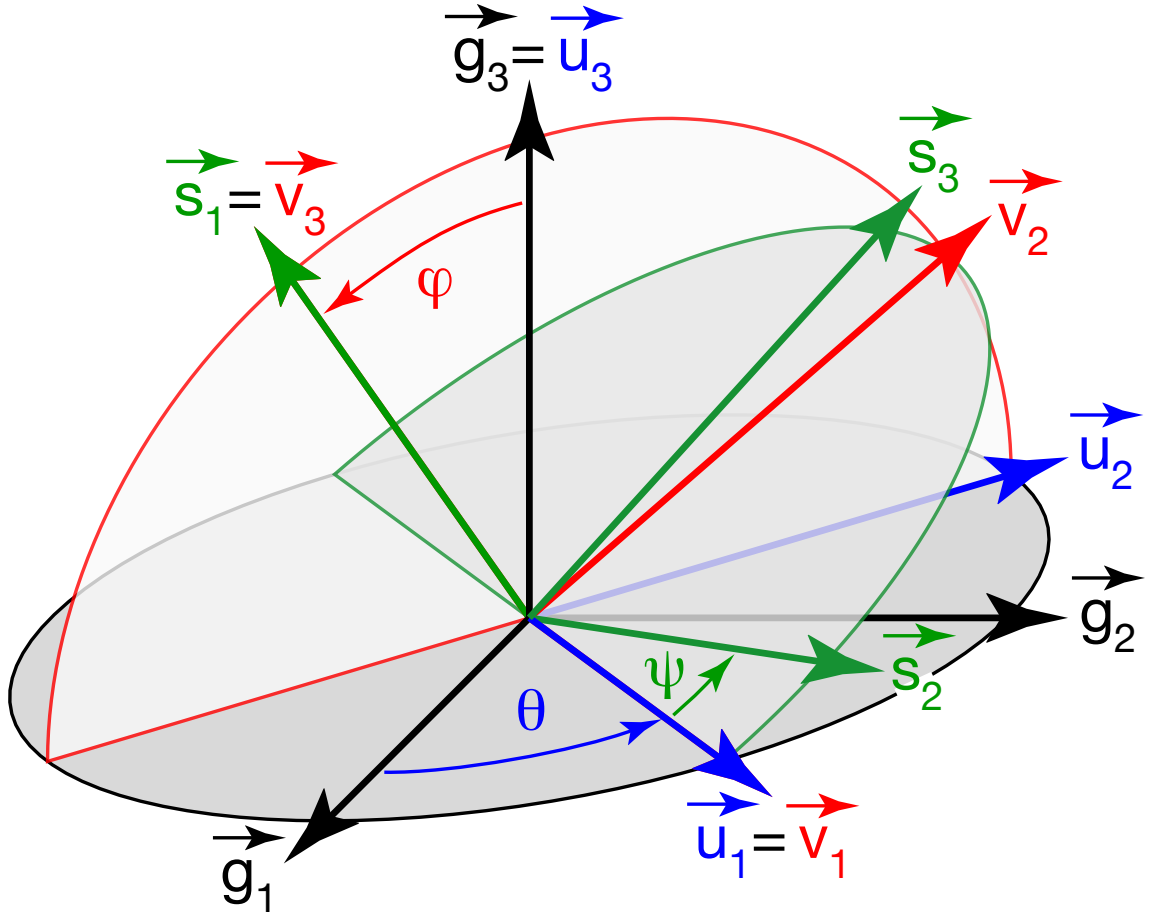
Figure 3.1: *Euler*'s (1767) angles transforming the geographical frame, $G = (\vec{g_1}, \vec{g_2}, \vec{g_3})$ into the principal stress frame $S = (\vec{s_1}, \vec{s_2}, \vec{s_3})$ through 3 successive rotations of angles $\theta, \varphi,$ and ψ. The intermediate stages are $\vec{u_1}, \vec{u_2}, \vec{u_3}$ and $\vec{v_1}, \vec{v_2}, \vec{v_3}$. After *Célérier* (1988).

3.3.2 Trend and plunge angles

Using the trend and plunge of $\vec{s_1}$, $\vec{s_2}$, and $\vec{s_3}$ is another way of defining the S frame. This representation is easier to interpret than Euler's angles. However, because the defintion of

S requires only 3 parameters, only 3 of the 6 trend and plunge parameters are independent. The angle ranges can be restricted to:

- Trend in $[0\,^\circ, 360\,^\circ]$
- Plunge in $[-90\,^\circ, 90\,^\circ]$

In geology directions are usually chosen downwards, so that plunge can be restricted to $[0\,^\circ, 90\,^\circ]$. Even though this will be accepted in input, FSA internal representation transform the input to build a right handed S frame with downgoing $\vec{s_1}$ and $\vec{s_3}$, so that the plunges $\vec{s_1}$ and $\vec{s_3}$ are within $[0\,^\circ, 90\,^\circ]$, but that of $\vec{s_2}$ is within $[-90\,^\circ, 90\,^\circ]$ in output.

3.4 Revisions of this chapter

|2016-11-02 |2016-05-11 |

Chapter 4

Data files: general requirements

2016-10-08

4.1 Introduction

This chapters describes a few common attributes of data files used by the Fsa program.

4.2 Fortran input/output conventions

Fsa is developed in Fortran and uses Fortran sequential input and output text files.

- The input/output files are ASCII files, i.e. plain text files without accentuated characters. If input files are prepared within a software other than a pure text editor, such as a word processor or a spreadsheet, they need be exported as text only files.

- During input, each reading statement normally focusses on one input line with the following conventions:

  - If all the data to be read within a line are found, the rest of the line is not read. The next input statement will seek its data in the next line. This implies that extra information can be added AFTER the required data without affecting the input.

  - If all the data to be read are not found within a line, the missing data will be sought in the next line. This implies that an incomplete line will be completed by the probably misinterpreted next line.

- There are two possible formats for input files: free or fixed formats. Free format is preferred and used as much as possible in Fsa. However, fixed formats are often required.

4.2.1 Fortran free format

- Reading rules
  - Data are separated by empty spaces or tabulations (more suited for spreadsheet).
  - Character strings MUST be delimited by single quotes, ', to be read properly.
- Possible file preparation
  - In a text editor or spreadsheet and saved as text only.
  - Tab separated text output is most convenient, as it is easy to read and can also be opened in a spreadsheet.

4.2.2 Fortran fixed format

- Reading rules
  - Numerical data and character strings are read within a specific column location. Column here means the number of characters (or spaces) counted from the beginning of the line.
  - No delimiters are necessary: character strings are delimited by their exact column location.
  - A column offset in a data line will result in misinterpreted data.
- Possible file preparation
  - In a text editor and saved as text only; each character position must be counted from the beginning of each line.

4.3 Operating system issues

4.3.1 Encoding

Text encoding systems that are compatible with ASCII should work. On MacOS X both Mac OS Roman and UTF-8 work.

4.3.2 End of line

The special character used to mark the end of line (EOL) in the input file must be consistent with the system used to run FSA (Table 4.1). If the end of line is not recognized, the whole input file may appear as a single line to the program. Problems tend to arise when the file is created in one operating system and transferred to another system where the program is run, or when the file is exported from a word processor or spreadsheet.

Table 4.1: End of line (EOL) coding. CR = Carriage Return; LF = Line Feed.

Operating system	End of line (EOL)
MacOS X	LF
Unix	LF
Windows	CRLF
MacOS Classic	CR

Using text, as opposed to binary, ftp transfer of data files between system should translate the end of line. Use a text editor that allows to check and modify end of line characteristics before running FSA on MacOS X with files coming from MacOS Classic or Windows systems, as this will usually require to change the end of line.

4.3.3 End of file

- Aways terminate the file with an empty line (extra line with no space). This avoids putting the end of file (EOF) tag in the last data line. In some systems, including MacOS X, such a situation can result in the last data line not being read.

- Always check that the number of data stored in the program is exactly the expected number of data. If one datum is missing, the above most likely applies.

4.4 Creating input files

Data files can be created with a text editor (recommended) or a word processor. Free format data files can also be created with a spreadsheet.

4.4.1 Text editors

Preparing an input file with a text editor has the advantage of directly creating a plain text file. There are then only two issues to deal with when saving the file:

1. check and eventually modify end of line coding, and

2. make sure the end of file is below the last data line.

Here is a list of text editors that allow to check and alter end of line and text encoding of text files:

- under MacOS X: TextWrangler, BBEdit, Smultron, and Plain Text Editor;
- under Windows: ConTEXT.

4.4.2   Spreadsheets

Input files that are read in free format can be prepared with a spreadsheet. There are then four issues to deal with:

1. exporting the file as tab delimited text,
2. making sure that character strings are enclosed within quotes for free format files,
3. checking and eventually correcting end of line coding, and
4. making sure the end of file is below the last data line.

The last three issues are best dealt with by importing the file in a text editor.

4.4.3   Word processors

Finally, input files can also be prepared with a word processor. Three issues must de dealt with:

1. exporting the file in plain text (tab delimited columns recommended),
2. checking and eventually correcting end of line coding, and
3. making sure the end of file is below the last data line.

Again, the last two issues are best dealt with by importing the file in a text editor.

4.5   Fsa input/output files

Even though FSA handles various types of input file, a preferred format, that will be called 'standard' is used as often as possible. This format was designed to be easily exchanged with spreadsheets.

4.5.1 Standard input/output file

4.5.1.1 Standard file structure

- Data files are ASCII files.
- They are made of a header followed by data lines.

4.5.1.2 Standard header

The standard header is made of two lines:

1. Title line: the first line contains the title.
2. Columns headers line: the second line contains the columns headers

The standard header is read in free format: title and column headers are character strings and need be delimited by single quotes ', so as to be read properly.

4.5.1.3 Standard data line

- All parameters for each datum are given in a single data line.
- Data line are read in free format. Parameters may be separated by empty spaces or tabs. Character strings need be delimited by single quotes '.

4.5.1.4 Standard file example

Example of a standard data file with 2 reals, 1 integer and 1 character string per data. Here are the 3 first lines of the file with two header lines and the first data line:

1. 'Title'
2. 'Parameter-1' 'Parameter-2' 'Parameter-3' 'Parameter-4'
3. 12000.6 2999.4567 245 'label-of-data1'

4.5.2 Non standard input/output file

4.5.2.1 Non standar header

Files with non standard header settings can often be read after adjusting

- the number of header lines to skip,

- the number of the line to read title from (0 if none), and

- the number of the line to read column headers from (0 if none)

in the input module dialog.

4.5.2.2 Non standard data line

- Cases with fixed format: exact column location is required and there are no delimiters.

4.6 Revisions of this chapter

|25-07-2003 |01-03-2004 |08-11-2004 |30-11-2004 |2007-11-21 |2010-10-06 |2016-10-08 |

Chapter 5

Fault and slip data files

2016-11-02

5.1 Introduction

Since version 19, FSA is designed to handle various types of fault and slip data such as faults and slickenlines (the default), earthquake focal mechanisms, and fractures without slip indicator. For each data type, the program can also handle various ways of recording them and various file formats. It is therefore necessary to distinguish data types from data format and to set both properly before reading any input file.

- Data type defines the amount of information in the input file and constrains the operations that the software will be allowed to do with these data.

- Data format indicates how the required information is presented in the file.

As a consequence, four consecutive steps must be followed in the input module:

1. Specification of the data type

2. Specification of the data file format

3. Specification of the data file, i.e., the file location and name

4. Reading of the data file

This chapter describes the data types and data file formats available in FSA versions ≥ 35.4. The correspondence between formats and types is summarized in Table 5.1.

Table 5.1: Fault slip data types and formats

Data types (ID)	Data formats		
	Aki & Richards strike, dip, rake	Etchecopar strike, dip, pitch/trend	Dip direction, dip, trend, plunge
Fault and slip (100)	SDR	EF EM	ADTP2I DAPT2I
Fault and slip with rake range (110)	SDRH		
Fault and slip with bedding (150)	SDRSD	EMB	
Original and restored fault and slip with bedding (200)	2(SDR)SD		
Fault plane solution (300)	SDR 2(SDR) CMT-dek-NP		
Fault plane solution and 3 coordinates (313)	SDR3C 2(SDR)3C CMT-dek-NP CMT-ndk-NP FPFIT HASH		
Plane (400)	SD	EFP EMP	DA
Plane and 1 coordinate (411)	SDC		DAC GF-CDA

5.2 Data types

Each data type is tagged in the software with an identification integer (ID) given in the left column of Table 5.1.

5.2.1 Plane

Definition: Plane orientation only. Can be used for fractures, faults without slip indicator, veins, foliations or beddings.

5.2.2 Plane and 1 space coordinate

Definition: Plane orientation with one associated space coordinate. This is useful for fracture or bedding measurements along a linear outcrop, such as a roadcut, or from a

borehole.

5.2.3 Fault and slip

Definition: Fault plane and slickenline orientation. This is the default type when starting Fsa.

5.2.4 Fault and slip with rake range

Definition: Fault plane with slip known within a rake range only.

5.2.5 Fault and slip with bedding

Definition: Fault plane, slickenline and associated bedding orientations.

5.2.6 Original fault and slip, rotated fault and slip, with bedding

Definition: Original fault plane, slickenline and associated bedding orientations together with fault plane and slickenline orientations restored for horizontal bedding. This is an output format only, that can be used after Fsa has restored orientations.

5.2.7 Fault plane solution

Definition: Earthquake fault plane solution. Given either as one nodal plane or as both nodal planes.

5.2.8 Fault plane solution and 3 space coordinates

Definition: Earthquake fault plane solution with full hypocenter location.

5.3   Data formats

5.3.1   Strike, dip, rake with Aki & Richards' convention

Here are grouped various formats that all represent fault and slip orientation by strike, dip, and rake with Aki & Richards' convention.

5.3.1.1   SDR: strike, dip, rake

- Purpose
  - For fault and slip data or one nodal plane of a fault plane solution.
- File structure
  - Standard file structure
- Data line structure
  - 3 real numbers in free format.
  - The 3 real numbers correspond to the strike, dip and rake in degrees with Aki & Richards' convention.
- Sample file
  - RD37_fs_sdr.txt

5.3.1.2   SD: strike, dip

- Purpose
  - For planar structure orientation data
- File structure
  - Standard file structure
- Data line structure
  - 2 real numbers in free format.
  - The 2 real numbers correspond to the strike and dip in degrees with Aki & Richards' convention.

5.3.1.3   SDC: strike, dip, z

- Purpose
  - For planar structure with 1 space coordinate orientation data
- File structure
  - Standard file structure
- Data line structure
  - 3 real numbers in free format.
  - The 3 real numbers correspond to the strike and dip in degrees with Aki & Richards' convention, and to the space coordinate, either distance along path (for outcrops) or depth (for boreholes).

5.3.1.4   SDR3C: strike, dip, rake, x, y, z

- Purpose
  - For fault plane solutions with 3 space coordinates
- File structure
  - Standard file structure
- Data line structure
  - 6 real numbers in free format.
  - The 6 real numbers correspond to strike, dip and rake in degrees with Aki & Richards' convention, and to the 3 space coordinates, (either x, y, z or longitude, latitude, depth)

5.3.1.5   2(SDR): 2•(strike, dip, rake)

- Purpose
  - For fault plane solutions where both nodal planes are given.
- File structure
  - Standard file structure
- Data line structure
  - 6 real numbers in free format.

– The 6 real numbers correspond to the strike, dip and rake for the first nodal plane followed by the strike, dip and rake for the second nodal planes. Angles are in degrees and follow Aki & Richards' convention.

5.3.1.6 2(SDR)3c: 2•(strike, dip, rake), x, y, z

- Purpose
    - For fault plane solutions with 3 space coordinates where both nodal planes are given.
- File structure
    - Standard file structure
- Data line structure
    - 9 real numbers in free format.
    - The 9 real numbers correspond to strike, dip and rake for the first nodal planes, followed by those for the second nodal plane, followed by the 3 space coordinates (either x, y, z, or longitude, latitude, depth). Strike, dip and rake are in degrees and follow Aki & Richards' convention.

5.3.1.7 SDRSD: strike, dip, rake, strike, dip

- Purpose
    - For fault and slip with bedding orientation data. The bedding plane orientation is measured at the same location as the fault. This can then be used to restore the structural orientations to the situation where bedding is horizontal.
- File structure
    - Standard file structure
- Data line structure
    - 5 real numbers in free format.
    - The 5 real numbers correspond to the strike, dip and rake of the fault and slip data and to the strike and dip of the bedding. All angles are in degrees and Aki & Richards' convention is used

5.3.1.8 2(SDR)SD: 2•(strike, dip, rake), strike, dip

- Purpose

- For original and restored fault and slip with bedding plane data. This format is used for output after restoration of the structural orientations to the situation with horizontal bedding.

- File structure

  - Standard file structure

- Data line structure

  - 8 real numbers in free format.

  - The 8 real numbers correspond to the strike, dip and rake of the original fault and slip data, to the strike, dip and rake of the restored fault and slip data, and to the strike, dip of the bedding. All angles are in degrees and Aki & Richards' convention is used.

5.3.1.9 SDRH: strike, dip, rake, half rake range

- Purpose

  - For fault and slip with rake range data.

- File structure

  - Standard file structure

- Data line structure

  - 4 real numbers in free format.

  - The 4 real numbers correspond to the strike, dip, rake, and half the uncertainty range in rake of the fault and slip data. All angles are in degrees and Aki & Richards' convention is used.

- Examples of rake ranges in Table 5.2.

Table 5.2: Rake uncertainty range

| Observed constraint on | | Rake | Rake | Half rake |
strike slip sense	dip slip sense	range		range
Senestral	None	[-90, 90]	0	90
None	Normal	[-180, 0]	-90	90
Senestral	Normal	[-90, 0]	-45	45

5.3.1.10 CMT-dek-NP

- Purpose

- Older format of the Harvard Centroid Moment Tensor catalog.

- Can be read either as fault plane solutions or as fault plane solutions with 3 coordinates.

- For input of the nodal planes information with or without location, depending on the selected type.

- File structure

  1. No header.

  2. Data lines: each datum correspond to 4 lines.

- Data line structure

  - Parameters are read in fixed format described in the CMT-dek documentation

5.3.1.11 CMT-ndk-NP

- Purpose

  - Current format of the Global Centroid Moment Tensor catalog.

  - Read as fault plane solutions with 3 coordinates.

  - For input of the nodal planes and location information.

- File structure

  1. No header.

  2. Data lines: each datum correspond to 5 lines.

- Data line structure

  - Parameters are read in fixed format described in the CMT-ndk documentation

5.3.1.12 FPFIT

- Purpose

  - Ouput format of the FPFIT program (*Reasenberg and Oppenheimer*, 1985).

  - Read as fault plane solutions with 3 coordinates.

- File structure

  1. No header.

  2. Data lines: each datum correspond to 1 line.

- Data line structure

– Parameters are read in fixed format described in the FPFIT documentation (*Reasenberg and Oppenheimer*, 1985).

5.3.1.13 HASH

- Purpose
    - Format of the SCEDC focal mechanism catalog for southern California (*Yang et al.*, 2012; *Hauksson et al.*, 2012).
    - Read as fault plane solutions with 3 coordinates.
- File structure
    1. No header.
    2. Data lines: each datum correspond to 1 line.
- Data line structure
    - Parameters are read in fixed format described in the SCEDC catalog.

5.3.2 Strike, dip, pitch/trend based on Etchecopar's Faille format

5.3.2.1 EF: original Etchecopar's Faille format

- Purpose
    - For field measurements of fault and slip data.
    - Combines strike, dip, pitch and strike, dip, trend field measurements into a single data file.
    - Sole format accepted by Etchecopar & Vasseur's program, FAILLE (*Etchecopar et al.*, 1981; *Etchecopar*, 1984).
    - Useful for legacy data.
- File structure
    1. Non standard single line header: the first line contains the title, read in fixed format.
    2. Data lines: each datum correspond to 1 line.
    3. The last line has number 450 in column 3-4-5, i.e. at the location of strike (Table 5.3), to indicate the end of data.
- Data line structure

- – each data line is
  - ∗ either of the type
    (strike, dip, dip quadrant, rake, rake quadrant, fault type, id)
  - ∗ or of the type
    (strike, dip, dip quadrant, slip trend, fault type, id).
  - – The data lines are read in fortran fixed format:
    FORMAT (T3,I3,T10,I2,T17,A1,T21,I2,T26,A1,T29,I3,T35,A1,T70,I3,T74,1A3).
    This implies that character strings are not delimited by quotes, but by their
    column location
  - – Parameters and their positions are described in Table 5.3 .
- • Sample file
  - – RD37_fs_ef.txt

Table 5.3: EF format data line (Etchecopar's FAILLE). (1) Column location refer to the position in the 80 characters line (col 1 to 80 for a data line: old punch card format). (2) Angles are integers and in degrees. (3) N, E, S, W are upper case, single character variables. N, E, S, W = North, East, South, West. (4) N, I, D, S are upper case, single character variables. N, I, D, S = Normal, Reverse (Inverse), Dextral, Sinistral. (5) In fsa/reafsd, if the rake quadrant string is blank (i.e., rake quadrant = ' ') and rake = 0 then slip azimuth is used. In the faille program this test is reversed: if the slip azimuth = 0 (or blank space) then the rake is used. Thus an azimuth = 0 slip is wrongly assumed to be a pitch = 0 slip. Conclusion: replace azimuth = 0 by azimuth = 180 when using faille.

Data	Type	Range	Comment	Column location (1)
strike	integer	[0, 360]	strike azimuth (2)	3-4-5
dip	integer	[0, 90]	dip angle (2)	10-11
dip quadrant	character	N,E,S,W	dip quadrant (3)	17
rake	integer	[0, 90]	rake or pitch angle (2,5)	21-22
rake quadrant	character	N,E,S,W	rake quadrant (3,5)	26
slip azimuth	integer	[0, 180]	slip azimuth (2,5)	29-30-31
fault type	character	N,I,D,S	fault type (4)	35
id	integer	[0, 999]	identifies the fault	70-71-72

5.3.2.2 EFP: original Etchecopar's Faille for plane only

- • Purpose
  - – Similar to format EF, but for plane only data.

- File structure

  - Same as EF.

- Data line structure

  - Same as EF, with the same position, but only (strike, dip, dip quadrant, id) are filled. Other parameters filled with blank spaces.

5.3.2.3   EM: Modified Etchecopar

- Purpose

  - For field measurements of fault and slip data.

  - This format is a modification of the Etchecopar's original EF format that

    * allows to prepare the data file in a spreadsheet,

    * is read in free format,

    * avoids the slip rake versus slip azimuth ambiguity,

    * but still corresponds closely to field measurements.

- File structure

  - Standard file structure

- Data line structure

  - Data lines are made of 3 real numbers, one integer number, and 3 character strings.

  - The data lines are read in fortran free format.

  - Each data line lists the following parameters in this order:
    strike, dip, dip quadrant, slip angle, slip quadrant, fault type, id.

  - Parameters are described in Table 5.4 .

- The data file can be prepared in a spreadsheet as follow:

  1. enter the data in a spreadsheet;

  2. save them as a text file;

  3. open the text file in a text editor or word processor and replace all occurrences of N,E,S,W,A,I,D by 'N','E','S','W','A','I','D' ;

  4. save again as text;

  5. verify end of line and end of file and alter them if needed (most easily done with a text editor);

34

6. save again as text: this is the input file.

- Sample file

  - RD37_fs_em.txt

Table 5.4: EM format data line (Modified Etchecopar). (1) Columns number here refer to spreadsheet columns, i.e., to the tab-separated entries in the text file. (2) Angles are real numbers and in degrees. (3) N, E, S, W are upper case, single character variables. N, E, S, W = North, East, South, West. (4) N, I, D, S are upper case, single character variables. N, I, D, S = Normal, Reverse (Inverse), Dextral, Sinistral. (5) Slip angle interpretation: if slip quadrant = N,E,S,W, then slip angle is the rake within [0,90]; if slip quadrant = A, then slip angle is the slip azimuth within [0,180].

Data	Type	Range	Comment	Column number (1)
strike	real	[0, 360]	strike azimuth (2)	1
dip	real	[0, 90]	dip angle (2)	2
dip quadrant	character	N,E,S,W	dip quadrant (3)	3
slip angle	real	[0, 180]	slip angle (2)	4
slip quadrant	character	N,E,S,W,A	rake quadrant (3) or azimuth tag (5)	5
fault type	character	N,I,D,S	fault type (4)	6
id	integer	[0, 999]	identifies the fault	7

5.3.2.4   EMP: Modified Etchecopar for plane only

- Purpose

  - Similar to format EM, but for planar structure orientation data.

- File structure

  - Standard file structure

- Data line structure

  - Data lines are made of 2 real numbers, one integer number, and 1 character strings.

  - The data lines are read in fortran free format.

  - Each data line lists the following parameters in this order:
    strike, dip, dip quadrant, id.

  - Parameters are described in Table 5.5 .

Table 5.5: EMP format data line (Modified Etchecopar for plane only). Same conventions as in Table 5.4.

Data	Type	Range	Comment	Column number
strike	real	[0, 360]	strike azimuth	1
dip	real	[0, 90]	dip angle	2
dip quadrant	character	N,E,S,W	dip quadrant	3
id	integer	[0, 999]	identifies the fault	4

5.3.2.5 EMB: Modified Etchecopar for fault slip with bedding

- Purpose
    - Similar to format EM, but for fault and slip with bedding orientation data.
- File structure
    - Standard file structure
- Data line structure
    - Data lines are made of 5 real numbers, one integer number, and 4 character strings.
    - The data lines are read in fortran free format.
    - Each data line lists the following parameters in this order:
      strike, dip, dip quadrant, slip angle, slip quadrant, fault type, id, bedding strike, bedding dip, bedding dip quadrant.
    - Parameters are described in Table 5.6 .

5.3.3 Dip direction, dip, trend, plunge

In these input formats where slip orientation is given by trend and plunge, measurements errors will usually place the slip vector slightly out of the fault plane. Rake is therefore computed by projecting the slip vector on the fault plane either vertically for low dip planes or horizontally for high dip planes. The FSA program also computes the angle, β, between slip vector and fault plane and issues

- a warning when $3\,° \leq \beta < 10\,°$ and
- an error message when $10\,° \leq \beta$

Table 5.6: EMB format data line (Modified Etchecopar for fault slip with bedding). Same conventions as in Table 5.4.

Data	Type	Range	Comment	Column number
strike	real	[0, 360]	strike azimuth	1
dip	real	[0, 90]	dip angle	2
dip quadrant	character	N,E,S,W	dip quadrant	3
slip angle	real	[0, 180]	slip angle	4
slip quadrant	character	N,E,S,W,A	rake quadrant or azimuth tag	5
fault type	character	N,I,D,S	fault type	6
id	integer	[0, 999]	identifies the fault	7
bedding strike	real	[0, 360]	strike azimuth	8
bedding dip	real	[0, 90]	dip angle	9
bedding dip quadrant	character	N,E,S,W	dip quadrant	10

5.3.3.1   DA: dip, dip direction

- Purpose
  - For planar structure orientation data.
  - Concise, fully numerical and unambiguous.
- File structure
  - Standard file structure
- Data line structure
  - 2 real numbers in free format.
  - The 2 real numbers correspond to the dip and dip direction in degrees.

5.3.3.2   DAC: dip, dip direction, z

- Purpose
  - For plane and 1 coordinate data.
  - Concise, fully numerical and unambiguous.
- File structure
  - Standard file structure
- Data line structure

– 3 real numbers in free format.

– The 3 real numbers correspond to the dip and dip direction in degrees, and to the space coordinate.

5.3.3.3   GF-CDA: Geoframe z, dip, dip direction

- Purpose
    - Format of the dip to ascii output file of Schlumberger Geoframe planar structure picks.
- File structure
    1. No header.
    2. Data lines: each datum correspond to 1 line.
- Data line structure
    - Parameters are read in fixed format.
    - Only the depth, dip and dip direction are read.

5.3.3.4   ADTP2I: Dip direction, dip, trend, plunge

- Purpose
    - For fault and slip data where slip direction is given by trend and plunge.
- File structure
    - Standard file structure
- Data line structure
    - 6 numbers in free format: 4 real numbers followed by 2 integer numbers.
    - The 6 numbers are read in free format and are ordered as follows :
        1. the fault plane dip direction in degrees (real number)
        2. the fault plane dip angle in degrees (real number)
        3. the slip vector trend (azimuth) in degrees (real number)
        4. the slip vector plunge in degrees (real number)
        5. a code within [1,4] for the movement type: 1 = reverse, 2 = normal, 3 = dextral, 4 = sinistral (integer number)
        6. an identification number for the datum (integer number)

5.3.3.5   DAPT2I: Dip, dip direction, plunge, trend

- Purpose
  - For fault and slip data where slip direction is given by trend and plunge.
  - Same as ADTP2I, but with different order in the data line
- File structure
  - Standard file structure
- Data line structure
  - Data lines are made of 6 numbers per data line in free format: 4 real numbers followed by 2 integer numbers.
  - The 6 numbers are read in free format and are ordered as follows :
    1. the fault plane dip angle in degrees (real number)
    2. the fault plane dip direction in degrees (real number)
    3. the slip vector plunge in degrees (real number)
    4. the slip vector trend (azimuth) in degrees (real number)
    5. a code within [1,4] for the movement type: 1 = reverse, 2 = normal, 3 = dextral, 4 = sinistral (integer number)
    6. an identification number for the datum (integer number)

5.4   Revisions of this chapter

|2002-06-21 |2003-07-30 |2008-04-09 |2008-12-01 |2008-12-10 |2013-10-22 |2016-10-08 |2016-11-02 |

Chapter 6

Stress data files

2016-11-02

6.1 Introduction

FSA can handle various types of stress data. For each data type, the program can also handle various ways of recording them and various file formats. It is therefore necessary to distinguish data types from data format and to set both properly before reading any input file.

- Data type defines the amount of information in the input file and constrains the operations that the software will be allowed to do with these data.

- Data format indicates how the required information is presented in the file.

As a consequence, four consecutive steps must be followed in the input module:

1. Specification of the data type

2. Specification of the data file format

3. Specification of the data file, i.e., the file location and name

4. Reading of the data file

This chapter describes the data types and data file formats available in FSA versions $\geq$ 35.4. The correspondence between formats and types is summarized in Table 6.1 .

Table 6.1: Stress data types and formats

Data types (ID)	Data formats
S by Euler's angles and r_0 (200)	3ER
S by Euler's angles, r_0, and 2 coordinates (202)	3ER2C
S by Euler's angles, r_0, and 3 coordinates (203)	3ER3C
S by azimuth and plunge and r_0 (250)	3(AP)R 2(AP)-PT
S by azimuth and plunge, r_0, and 2 coordinates (252)	3(AP)R2C
S by azimuth and plunge, r_0, and 3 coordinates (253)	3(AP)R3C CMT-dek-PBT CMT-ndk-PBT 2(AP)3C-PT

6.2   Data types

Each data type is tagged in the software with an identification integer (ID) given in the left column of Table 6.1.

For all types discussed below, only the reduced stress tensor, introduced in section 3.2 and equations 3.1 and 3.6, is involved. It is defined by r_0 (equation 3.4) and the principal stress directions, i.e., the orientation of the $S = (\vec{s_1}, \vec{s_2}, \vec{s_3})$ frame (defined in section 3.2 and Table ??) with respect to the geographical frame, G (defined in section 1.4 and Table ??). This orientation can be defined

- either by 3 Euler's angles that transform G into S (section 3.3.1 and Fig 3.1)

- or by the 6 trend and plunge angles of $\vec{s_1}, \vec{s_2}$, and $\vec{s_3}$ (section 3.3.2).

6.2.1   S by Euler's angles and r_0

Definition: Reduced stress tensor given by Euler's angles and r_0.

6.2.2   S by Euler's angles, r_0 and 2 coordinates

Definition: Reduced stress tensor given by Euler's angles and r_0 with 2 location coordinates. The coordinates can be either cartesian coordinates, x and y, in a frame of reference or spherical coordinates, longitude and latitude.

6.2.3 S by Euler's angles, r_0 and 3 coordinates

Definition: Reduced stress tensor given by Euler's angles and r_0 with 3 location coordinates. The coordinates can be either cartesian coordinates, x, y and z, in a frame of reference or spherical coordinates, longitude, latitude and depth.

6.2.4 S by azimuth and plunge and r_0

Definition: Reduced stress tensor given by the azimuth and plunge of the 3 principal stress directions $\vec{s_1}, \vec{s_2}$, and $\vec{s_3}$ and by r_0. Note that because the defintion of S requires only 3 parameters, only 3 of the 6 trend and plunge parameters are independent.

6.2.5 S by azimuth and plunge, r_0 and 2 coordinates

Definition: Reduced stress tensor given by the azimuth and plunge of the 3 principal stress directions $\vec{s_1}, \vec{s_2}$, and $\vec{s_3}$ and by r_0 with 2 location coordinates. The coordinates can be either cartesian coordinates, x and y, in a frame of reference or spherical coordinates, longitude and latitude.

6.2.6 S by azimuth and plunge, r_0 and 3 coordinates

Definition: Reduced stress tensor given by the azimuth and plunge of the 3 principal stress directions $\vec{s_1}, \vec{s_2}$, and $\vec{s_3}$ and by r_0 with 3 location coordinates. The coordinates can be either cartesian coordinates, x, y and z, in a frame of reference or spherical coordinates, longitude, latitude and depth.

6.3 Data formats

6.3.1 Euler's angles

Here are grouped various formats that use Euler's angles to define the the principal stress directions.

6.3.1.1 3ER: three Euler's angles and r_0

- Purpose
  - For reduced stress tensor data given by Euler's angles and r_0.

- File structure
  - Standard file structure
- Data line structure
  - 4 real numbers in free format.
  - The 4 real numbers correspond to three Euler's angles θ, φ, ψ, and r_0. Angles are in degrees
- Sample file
  - sv_st_3er.txt

6.3.1.2 3ER2C: three Euler's angles, r_0, and 2 coordinates

- Purpose
  - For reduced stress tensor data given by Euler's angles, r_0, and 2 coordinates for location.
  - This format is obsolescent and the similar format with 3 coordinates should be used instead.
- File structure
  - Standard file structure
- Data line structure
  - 6 real numbers in free format.
  - The 6 real numbers correspond to three Euler's angles, θ, φ, ψ, r_0, and the two coordinates: either x, y or longitude, latitude. Angles are in degrees

6.3.1.3 3ER3C: three Euler's angles, r_0, and 3 coordinates

- Purpose
  - For reduced stress tensor data given by Euler's angles, r_0, and 3 coordinates for location.
- File structure
  - Standard file structure
- Data line structure
  - 7 real numbers in free format.

– The 7 real numbers correspond to three Euler's angles, θ, φ, ψ, r_0, and the three coordinates: either x, y, z or longitude, latitude, depth. Angles are in degrees

6.3.2 Azimuth and plunge

Here are grouped various formats that use azimuth and plunge to define the the principal stress directions.

6.3.2.1 3(AP)R: 3•(azimuth, plunge), r_0

- Purpose
  - For reduced stress tensor data given by azimuth, plunge and r_0.
- File structure
  - Standard file structure
- Data line structure
  - 7 real numbers in free format.
  - The 7 real numbers correspond to the azimuth, plunge of $\vec{s_1}$, followed by the azimuth, plunge of $\vec{s_2}$ and $\vec{s_3}$, and r_0. Angles are in degrees
- Sample file
  - sv_st_3(ap)r.txt

6.3.2.2 3(AP)R2C: 3•(azimuth, plunge), r_0 and 2 coordinates

- Purpose
  - For reduced stress tensor data given by azimuth, plunge, r_0, and 2 coordinates.
  - This format is obsolescent and the similar format with 3 coordinates should be used instead.
- File structure
  - Standard file structure
- Data line structure
  - 9 real numbers in free format.
  - The 9 real numbers correspond to the azimuth, plunge of $\vec{s_1}$, $\vec{s_2}$, $\vec{s_3}$, r_0, and the two coordinates: either x, y or longitude, latitude. Angles are in degrees

6.3.2.3   3(AP)R3C: 3•(azimuth, plunge), r_0 and 3 coordinates

- Purpose
  - For reduced stress tensor data given by azimuth, plunge, r_0, and 3 coordinates.
- File structure
  - Standard file structure
- Data line structure
  - 10 real numbers in free format.
  - The 10 real numbers correspond to the azimuth, plunge of $\vec{s_1}$, $\vec{s_2}$, $\vec{s_3}$, r_0, and the three coordinates: either x, y, z or longitude, latitude, depth. Angles are in degrees

6.3.2.4   2(AP)-PT: 2•(azimuth, plunge)

- Purpose
  - For seismic catalog where only P and T axes are given. The two axes are completed with B to build S, and with an arbitrary r_0 to build a reduced stress tensor of azimuth, plunge, r_0 type.
- File structure
  - Standard file structure
- Data line structure
  - 4 real numbers in free format.
  - The 4 real numbers correspond to the azimuth, plunge of P, followed by the azimuth, plunge of T. Angles are in degrees

6.3.2.5   2(AP)3C-PT: 2•(azimuth, plunge) and 3 coordinates

- Purpose
  - For seismic catalog where only P and T axes are given with 3 coordinates. The two axes are completed with B to build S, then with an arbitrary r_0, and the coordinates with to build a reduced stress tensor of azimuth and plunge, r_0 and 3 coordinates type.
- File structure
  - Standard file structure

- Data line structure

  - 7 real numbers in free format.

  - The 7 real numbers correspond to the azimuth, plunge of P, and T, and the three coordinates: either x, y, z or longitude, latitude, depth. Angles are in degrees.

6.3.2.6 CMT-dek-PBT

- Purpose

  - Older format of the Harvard Centroid Moment Tensor catalog.

  - P, B and T are read from the input file to build S, and an arbitrary value for r_0 is generated to build a reduced stress tensor of azimuth, plunge, r_0, and 3 coordinates type.

- File structure

  1. No header.

  2. Data lines: each datum correspond to 4 lines.

- Data line structure

  - Parameters are read in fixed format described in the CMT-dek documentation

6.3.2.7 CMT-ndk-PBT

- Purpose

  - Current format of the Global Centroid Moment Tensor catalog.

  - P, B and T are read from the input file to build S, and an arbitrary value for r_0 is generated to build a reduced stress tensor of azimuth, plunge, r_0, and 3 coordinates type.

- File structure

  1. No header.

  2. Data lines: each datum correspond to 5 lines.

- Data line structure

  - Parameters are read in fixed format described in the CMT-ndk documentation

6.4 Revisions of this chapter

|2000-09-04 |2003-09-10 |2008-04-09 |2016-11-02 |

Chapter 7

How to refer to Fsa and relevant references

2020-06-15

7.1 Introduction

This chapter discusses how to refer to FSA and recalls relevant references

7.2 How to refer to Fsa

If you publish results obtained with FSA, it would be appreciated that you referred to:

- *Etchecopar et al.* (1981) who introduced the random search method, with the possibility to account for only part of the data in the case of multiphase data, that is used in FSA;

- *Heuberger et al.* (2010) or *Burg et al.* (2005) who describe the methods implemented in FSA and show examples of application;

- the software version and its location as:
  Celerier, B., YYYY, FSA: Fault & Stress Analysis software, version XX.X,
  http://www.celerier.gm.univ-montp2.fr/software/dcmt/fsa/fsa.html.
  where XX.X and YYYY are the version and year of the software used that can be found in 2 places :

  - they are displayed in the console when the program starts, and

  - they are printed at the top of all plots.

7.3 Other relevant references

Below are a few additional relevant references ordered by subjects of interest.

- The random search method implemented in FSA: *Etchecopar et al.* (1981); *Etchecopar* (1984).

- Original definition of $\phi = \frac{\sigma_2 - \sigma_3}{\sigma_1 - \sigma_3}$: *Angelier* (1975).

- Definition of $r_0 = \frac{\sigma_1 - \sigma_2}{\sigma_1 - \sigma_3}$ used in FSA: *Célérier* (1988); *Tajima and Célérier* (1989); *Célérier* (1995, 2008).

- Definition of $s_0 = \frac{\sigma_1 - \sigma_3}{\sigma_1}$ used in FSA: *Célérier* (1988); *Tajima and Célérier* (1989); *Célérier* (2008).

- Geometry of the optimal stress tensor for a single fault and slip datum: *Compton* (1966); *Etchecopar* (1984); *Célérier* (1988, 2008).

- Triangular representation of stress tensor axes: *Frohlich and Apperson* (1992); *Frohlich* (1992, 2001); Appendix B of *Célérier* (2008); *Célérier* (2010).

- The evaluation of friction conditions: Appendix A of *Burg et al.* (2005).

- The inversion of fault data with slip sense information only (note that, whereas the general idea originates from these papers, the inversion method implemented in FSA is different from that proposed in these papers): *Lisle et al.* (2001); *Orife et al.* (2002).

- Quality criteria for solutions in the case of polyphased data: Appendix A of *Heuberger et al.* (2010).

- Examples of application of FSA to fault and slip data: *Zeilinger et al.* (2000); *Célérier and Séranne* (2001); *Burg et al.* (2005); *Federico et al.* (2009, 2010); *Heuberger et al.* (2010); *Kounov et al.* (2010, 2011); *Titus et al.* (2002); *Dolati and Burg* (2013); *Federico et al.* (2014).

- Examples of application of FSA to focal mechanism data: *Provost and Houston* (2001, 2003a,b); *Célérier* (2008); *Dolati and Burg* (2013); *Bauve et al.* (2014); *Plateaux et al.* (2014); *Rigo et al.* (2015).

- Examples of application of FSA to structural measurements in boreholes: *De Larouzière et al.* (1999); *Célérier et al.* (2002); *Louvel et al.* (2002)

7.4 Revisions of this chapter

|2020-06-15|

Chapter 8

Fsa revision history

2020-06-15

8.1 Fsa versions history

FSA has been continuously evolving since an early prototype made in summer 1991. Originally developed on SUN workstations, it was ported to MacOS Classic, then to MacOS X. It has also been partially ported to Windows. Version history is summarized in Table 8.1.

Table 8.1: FSA program versions

Version	Date	Comments
37.4	8 May 2020	Add labels to s_0 lines in Mohr's representation.
37.3	19 November 2019	Clarify nodal plane choice in menus.
37.2	27 July 2019	Improve data description menus.
37.1	8 April 2019	Upgrade fault and stress data outputs and fault data display.
37.0	30 May 2018	Terminate upgrade of input of fault data as dip direction, dip, trend, plunge to output of a clearer and more complete error listing.
36.9	23 May 2018	Begin upgrade of input of fault data as dip direction, dip, trend, plunge to output of a clearer and more complete error listing.
36.8	18 January 2018	Terminate upgrade of math libraries.
36.7	25 July 2017	Upgrade plot landscape/portrait set up.
36.6	14 March 2017	Begin upgrade of math libraries.
36.5	29 November 2016	Modify axis range in tensor optimisation plots.

Table 8.1: (continued)

Version	Date	Comments
36.4	17 November 2016	Output of azimuth and plunge of slip vectors for FPS+3D coord and CPS+3D coord. Fix frame of slip trend rose diagram.
36.3	20 October 2016	Changes in menus and dialogs.
36.2	10 October 2016	Data format names and labels reorganized and documented.
36.1	27 May 2016	More use of color for fs in analysis.
36.0	25 May 2016	Use more efficient stereos for fs in analysis. Step 2: with color.
35.5	19 May 2016	Use more efficient stereos for fs in analysis. Step 1: without color.
35.4	15 July 2015	Dip, dip direction, plunge, trend input for fs.
35.3	27 February 2015	Fault plane only data output.
35.2	5 July 2013	Control on id in Breddin's plots.
35.1	2 June 2013	Add slip trend and plunge histograms.
35.0	12 Avril 2013	Fault and slip display upgrade: menu change, more plot options.
34.5	9 Avril 2013	Adapt axes to larger number of data (>100 000); wider console.
34.4	8 March 2013	More consistent mapping symbols.
34.3	26 February 2013	Adapt outputs to larger number of data (>100 000).
34.2	17 November 2012	Stereographic projection upgrade.
34.1	26 April 2012	Run time information upgrade.
34.0	11 November 2011	More use of improved stereographic projection.
33.9	10 November 2011	More control on axes set up.
33.8	1 March 2011	More mapping contours formats.
33.7	24 January 2011	Upgrade of analysis tabulated output.
33.6	14 May 2010	Quartz library interface update.
33.5	27 April 2010	Add beach ball plot of fault plane solutions.
33.4	21 April 2010	Add HASH (*Hauksson et al.*, 2012; *Yang et al.*, 2012) input for fault plane solutions.
33.3	29 January 2010	X-Y grids for maps.
33.2	30 November 2009	Direct computation of P,B,T from nodal planes.
33.1	24 November 2009	Mapping faults and slip vectors.
33.0	12 October 2009	Upgrade triangular diagrams: more projections, improved axes.
32.4	06 September 2009	Improve histograms axes.
32.3	04 September 2009	Upgrade histogram library.
32.2	18 May 2009	Optional color coding and graphic output (345/346) for analysis, map clipping, alternate axis symbol for stereographic projections standardized.

Table 8.1: (continued)

Version	Date	Comments
32.1	22 April 2009	Add computation of optimal conjugate planes from stress tensor orientation and input of focal mechanisms given by P and T axes only.
32.0	1 April 2009	Shorten inversion calculations.
31.1	19 March 2009	Plot librairies upgrade.
31.0	27 February 2009	Conjugate planes with slip data type added.
30.5	17 December 2008	Slip trend, plunge input and verification that slip is within the fault plane.
30.4	16 December 2008	Slip trend, plunge input.
30.3	01 December 2008	Slip trend, plunge output.
30.2	07 May 2008	P, B, T input.
30.1	10 April 2008	Inversion parameters menu upgrade.
30.0	28 March 2008	More coastline files for mapping.
29.9	18 February 2008	Axes upgrade.
29.8	09 January 2008	Input file error management upgrade. Checkerbox plot legend. AzShmax normalisation.
29.7	26 November 2007	Histogram library upgrade.
29.6	26 September 2007	Reorganize static libraries.
29.5	01 September 2007	Fix axis label in single fault analysis.
29.4	20 August 2007	Modify stress tensor set up and input.
29.3	05 August 2007	Modify fault and slip set up and input.
29.2	12 June 2007	Random fault and slip generation.
29.1	12 March 2007	Superposed histograms: stable solution.
29.0	07 January 2007	Axes upgrade.
28.8	05 October 2006	Add tabulated Etchecopar format to fault slip and bedding input.
28.7	25 July 2006	Superposed histograms: temporary solution.
28.6	14 June 2006	Plunge compensated histograms.
28.5	12 May 2006	Extra Mohr space friction line options.
28.4	18 April 2006	Extra stress directions mapping options.
28.3	01 December 2005	MacOSX Quartz version. Axis library upgrade.
28.2	01 September 2005	Comprehensive analysis spreadsheet friendly output file.
28.1	22 August 2005	Basic analysis output file.
28.0	07 March 2005	Stress projection for mapping.
27.6	27 January 2005	Stereo upgrade for large number of data.
27.5	09 June 2004	Rose diagrams.
27.4	02 June 2004	Enhance axis and analysis.
27.3	17 February 2004	Internal reorganisation.
27.2	10 November 2003	Single fault - single stress tensor analysis. More flexible axis library.
27.1	04 November 2003	Internal reorganisation.

Table 8.1: (continued)

Version	Date	Comments
27.0	31 October 2003	Optimal stress.
26.8	08 October 2003	Single plane FPS input, stereos upgrade, rake plots.
26.7	04 September 2003	Axis library upgrade.
26.6	07 July 2003	Separate stereos for explained and unexplained data. Friction lines for $s_0 = 0.68, 0.8, 1.0$.
26.5	20 March 2003	Add error function = max of errors.
26.4	02 December 2002	Add inversion with rake range.
26.3	17 November 2002	Optimization of solutions.
26.2	05 November 2002	More analysis options.
26.1	26 October 2002	Projection library upgrade.
26.0	24 October 2002	Triangular diagram upgrade. Stress id.
25.2	11 October 2002	Add tectonic regime plot.
25.1	03 September 2002	Projection library upgrade.
25.0	12 July 2002	Add stress tensor location and stress axis horizontal projection mapping.
24.4	20 June 2002	Stress tensor parameters histograms. Normalized angles.
24.3	11 June 2002	More fault plane input format (ef,em).
24.2	13 December 2001	More color options.
24.1	28 November 2001	Improved histogram axis.
24.0	18 August 2001	Add slip sense only inversion, as in *Lisle et al.* (2001).
23.2	15 June 2001	Add stress tensor display: stereos and *Frohlich*'s (1992; 2001) triangular diagrams.
22.0	06 June 2001	Fault plane solution (FPS) input, display, inversion (both or best), and analysis. Maximum set to 500 fps x 300 tensors. Calculations take more advantage of the reduced stress tensor matrix structure and are therefore 170% faster.
21.2	31 October 2000	Add command files and fault plane (without slip) input & display. Geoframe format input for borehole fracture analysis.
20.7	04 September 2000	Stress tensor input and output. Note that the stress file header is now only 2 lines long, as in FSA18.8, but as opposed to FSA18.7 and older where it is 3 lines long.
20.5	02 February 2000	Stress & fault analysis.
20.4	05 January 2000	Random tensor search.
20.3	06 November 1999	New stress tensor structure.
20.2	30 May 1999	Update data type.
20.1	27 May 1999	Update histograms.
20.0	14 May 1999	New histograms library.
19.2	31 January 1999	Rotates fault data around an horizontal axis.

Version	Date	Comments
19.1	29 December 1998	Reads + displays fault data.
19.0	13 May 1998	Begin development of a new thread based on a new data structure. New fault data structure implemented (no stress tensor yet).
18.9	22 May 2001	Calculations take more advantage of the reduced stress tensor matrix structure and are therefore 170% faster. After this version, all further development is done in the new thread starting at FSA19.0 because FSA22.0 already has more functionalities than FSA18.9 in particular for focal mechanisms. However, this version remains available because of a few of its functions that are not yet included in the newer versions.
18.8	04 September 2000	Stress tensor file format header changed from 3 lines to 2 lines. Note that old stress tensor files generated by FSA18.7 can still be read by changing the number of header lines to skip from 2 to 3.
18.7	06 March 2000	Introduces command files to automatize processing. Upgrade synthetic faults generation.
18.6	29 November 1999	Macintosh version: portrait set up option for -qdraw allows to keep the window from covering all the screen.
18.6	8 November 1999	Plot up to 1000 data. Revised PostScript: all 3 options (Compressed, NeWS and Illustrator v.2) should open with Adobe Illustrator. Best choices are NeWS (Default) or Compressed (smaller files but same quality as NeWS).
18.6	13 September 1999	Good news: FSA18.6 can read up to 1000 fault data instead of 300 in previous versions. Bad news: for Macintosh version, FSA18.6 needs around 9.5MB of RAM instead of 3.5MB in previous versions.
18.5	11 June 1999	ASCII output of analysis.
18.4	20 April 1999	More tensor output formats.
18.3	15 April 1999	Changes in graphical display. More tensor output formats. The Macintosh version is compiled with a higher degree of backgrounding. It is expected to be 25% slower but it let you work with other applications while it is running. This may also avoid the problem caused when Eudora tries to check mail while FSA is running, that could result in system crashes in previous versions.
18.2	10 December 1997	Add synthetic rakes.

Table 8.1: (continued)

Version	Date	Comments
18.1	3 November 1997	Upgrade Mohr's frame.
18.0	30 October 1997	Add tensor search and optimization on a % of the data.
17.0	29 October 1997	Add fault data display and simplify PostScript file management. It is now easier to close and reopen a new PostScript file to avoid overlays.
16.3	19 September 1997	Continue improving plot file management.
16.2	15 September 1997	Improve plot file management.
16.1	19 June 1997	Add run time information.
16.0	14 May 1997	Add Mohr circle analysis. New PowerPC optimized version for Macintosh.
15.2	30April 1997	Tensor labels.
15.1	10 February 1997	Add synthetics and tabulated Etchecopar format.
15.0	7 May 1996	Change stress tensor data structure. The program takes its current name: Fsa.
14.3[1]	19 April 1996	Add output of stress data
14.2[1]	18 April 1996	Add input of stress data
14.1[1]	10 April 1996	Add output of fault and slip data
14.0[1]	4 March 1996	Analysis decoupled from random search
13.0[1]	25 December 1995	Add single fault and tensor analysis.
12.0[1]	12 October 1995	Add optimal stress.
11.0[1]	4 October 1995	Internal upgrade.
10.0[1]	3 October 1995	Upgrade calculations and analysis.
9.0[1]	29 July 1995	Upgrade graphics.
8.0[1]	21 July 1995	Upgrade calculations and graphics.
7.0[1]	10 August 1993	SunOS with GKS port.
6.0[1]	22 July 1992	MacOS Classic port.
6.0[1]	6 August 1991	Improve and test calculations. Succesfully tested against Etchecopar's Faille.
5.0[1]	31 July 1991	Improve and test calculations. Extend graphics.
4.0[1]	26 July 1991	Improve and test calculations. Extend graphics.
3.0[1]	16 July 1991	Improve and test calculations. Extend graphics.
2.0[1]	13 July 1991	Add graphics using Sun CGI.
1.0[1]	9 July 1991	First prototype, Fsi, on SunOS. Input of fault and slip data, random tensor search, selection and output of the best stress tensor. No graphics.

---

[1]The program was named Fsi from versions 1.0 to 15.0

8.2   Revisions of this chapter

|2017-03-03|2017-03-07|2017-03-27|2020-06-15|

Bibliography

Aki, K., and P. G. Richards (1980), *Quantitative seismology; Theory and methods*, vol. I, 557 pp., W.H. Freeman and Company, San Francisco.

Aki, K., and P. G. Richards (2002), *Quantitative seismology - Second Edition*, 700 pp., University Science Books, Sausalito, California.

Angelier, J. (1975), Sur l'analyse de mesures recueillies dans des sites faillés: l'utilité d'une confrontation entre les méthodes dynamiques et cinématiques, *C. R. Acad. Sci., Série D, 281*, 1805–1808.

Bauve, V., R. Plateaux, Y. Rolland, G. Sanchez, N. Bethoux, B. Delouis, and R. Darnault (2014), Long-lasting transcurrent tectonics in SW Alps evidenced by Neogene to present-day stress fields, *Tectonophysics, 621*, 85 – 100, doi:10.1016/j.tecto.2014.02.006.

Burg, J.-P., B. Célérier, N. M. Chaudhry, M. Ghazanfar, F. Gnehm, and M. Schnellmann (2005), Fault analysis and paleostress evolution in large strain regions: methodological and geological discussion of the southeastern Himalayan fold-and-thrust belt in Pakistan, *Journal of Asian Earth Sciences, 24*(4), 445 – 467, doi:10.1016/j.jseaes.2003.12.008.

Célérier, B. (1988), How much does slip on reactivated fault plane constrain the stress tensor ?, *Tectonics, 7*(6), 1257–1278, doi:10.1029/TC007i006p01257.

Célérier, B. (1995), Tectonic regime and slip orientation of reactivated faults, *Geophysical Journal International, 121*(1), 143–191, doi:10.1111/j.1365-246X.1995.tb03517.x\&10.1111/j.1365-246X.1995.tb07021.x.

Célérier, B. (2008), Seeking Anderson's faulting in seismicity: a centennial celebration, *Review of Geophysics, 46*(4), RG4001, 1–34, doi:10.1029/2007RG000240.

Célérier, B. (2010), Remarks on the relationship between the tectonic regime, the rake of the slip vectors, the dip of the nodal planes, and the plunges of the P, B, and T axes of earthquake focal mechanisms, *Tectonophysics, 482*(1-4), 42–49, doi:10.1016/j.tecto.2009.03.006.

Célérier, B., and M. Séranne (2001), Breddin's graph for tectonic regimes, *Journal of Structural Geology, 23*(5), 789–801, doi:10.1016/S0191-8141(00)00140-1\&10.1016/S0191-8141(01)00058-X.

Célérier, B., V. Louvel, B. Le Gall, V. Gardien, and P. Huchon (2002), Presentation and structural analysis of FMS electrical images in the northern margin of the Woodlark Basin, in *Proceedings of the Ocean Drilling Program, Scientific Results*, vol. 180, edited by B. Taylor, P. Huchon, and A. Klaus, pp. 1–159, Ocean Drilling Program, College Station, Texas, doi:10.2973/odp.proc.sr.180.177.2002.

Célérier, B., A. Etchecopar, F. Bergerat, P. Vergely, F. Arthaud, and P. Laurent (2012), Inferring stress from faulting: from early concepts to inverse methods, *Tectonophysics*, *581*, 206–219, doi:10.1016/j.tecto.2012.02.009.

Compton, R. R. (1966), Analyses of Pliocene-Pleistocene deformation and stresses in northern Santa Lucia Range, California, *Geological Society of America Bulletin*, *77*(12), 1361–1379, doi:10.1130/0016-7606(1966)77[1361:AOPDAS]2.0.CO;2.

De Larouzière, F. D., P. A. Pézard, M. C. Comas, B. Célérier, and C. Vergniault (1999), Structure and tectonic stresses in metamorphic basement, Site 976, Alboran sea, in *Proceedings of the Ocean Drilling Program, Scientific Results*, vol. 161, edited by R. Zahn, M. C. Comas, and A. Klaus, pp. 319–329, Ocean Drilling Program, College Station, Texas, doi:10.2973/odp.proc.sr.161.212.1999.

Dolati, A., and J. P. Burg (2013), Preliminary fault analysis and paleostress evolution in the Makran fold-and-thrust belt in Iran, in *Lithosphere Dynamics and Sedimentary Basins: The Arabian Plate and Analogues*, edited by K. Al Hosani, F. Roure, R. Ellison, and S. Lokier, pp. 261–277, Springer Berlin Heidelberg, doi:10.1007/978-3-642-30609-9_13.

Etchecopar, A. (1984), Étude des états de contrainte en tectonique cassante et simulations de déformations plastiques (approche mathématique). Thèse d'État, Ph.D. thesis, Université des Sciences et Techniques du Languedoc.

Etchecopar, A., G. Vasseur, and M. Daignieres (1981), An inverse problem in microtectonics for the determination of stress tensors from fault striation analysis, *Journal of Structural Geology*, *3*, 51–65.

Euler, L. (1767), Du mouvement d'un corps solide quelconque lorsqu'il tourne autour d'un axe mobile, *Mémoires de l'Académie des sciences de Berlin*, *[16], (1760)*, 176–227.

Federico, L., C. Spagnolo, L. Crispini, and G. Capponi (2009), Fault-slip analysis in the metaophiolites of the Voltri massif: constraints for the tectonic evolution at the Alps/Apennine boundary, *Geological Journal*, *44*(2), 225–240, doi:10.1002/gj.1139.

Federico, L., L. Crispini, and G. Capponi (2010), Fault–slip analysis and transpressional tectonics: A study of Paleozoic structures in northern Victoria Land, Antarctica, *Journal of Structural Geology*, *32*(5), 667 – 684, doi:10.1016/j.jsg.2010.04.001.

Federico, L., L. Crispini, A. Vigo, and G. Capponi (2014), Unravelling polyphase brittle tectonics through multi-software fault-slip analysis: The case of the Voltri Unit, Western Alps (Italy), *Journal of Structural Geology*, *68*, 175 – 193, doi:10.1016/j.jsg.2014.09.011.

Frohlich, C. (1992), Triangle diagrams: ternary graphs to display similarity and diversity of earthquake focal mechanisms, *Physics of the Earth and Planetary Interiors*, *75*(1), 193–198, doi:10.1016/0031-9201(92)90130-N.

Frohlich, C. (2001), Display and quantitative assessment of distributions of earthquake focal mechanisms, *Geophysical Journal International*, *144*(2), 300–308, doi:10.1046/j.1365-246x.2001.00341.x.

Frohlich, C., and K. D. Apperson (1992), Earthquake focal mechanisms, moment tensors, and the consistency of seismic activity near plate boundaries, *Tectonics*, *11*(2), 279–296, doi:10.1029/91TC02888.

Hauksson, E., W. Yang, and P. M. Shearer (2012), Waveform relocated earthquake catalog for southern California (1981 to june 2011), *Bulletin of the Seismological Society of America*, *102*(5), 2239–2244, doi:10.1785/0120120010.

Heuberger, S., B. Célérier, J. P. Burg, N. M. Chaudhry, H. Dawood, and S. Hussain (2010), Paleostress regimes from brittle structures of the Karakoram-Kohistan suture zone and surrounding areas of NW Pakistan, *Journal of Asian Earth Sciences*, *38*(6), 307–335, doi:10.1016/j.jseaes.2010.01.004.

Kounov, A., D. Seward, J.-P. Burg, D. Bernoulli, Z. Ivanov, and R. Handler (2010), Geochronological and structural constraints on the cretaceous thermotectonic evolution of the kraishte zone, western bulgaria, *Tectonics*, *29*(2, TC2002), 1–19, doi:10.1029/2009TC002509.

Kounov, A., J.-P. Burg, D. Bernoulli, D. Seward, Z. Ivanov, D. Dimov, and I. Gerdjikov (2011), Paleostress analysis of Cenozoic faulting in the Kraishte area, SW Bulgaria, *Journal of Structural Geology*, *33*(5), 859 – 874, doi:10.1016/j.jsg.2011.03.006.

Lisle, R., T. Orife, and L. Arlegui (2001), A stress inversion method requiring only fault slip sense, *Journal of Geophysical Research: Solid Earth*, *106*(B2), 2281–2289, doi:10.1029/2000JB900353.

Louvel, V., B. Le Gall, B. Célérier, V. Gardien, and P. Huchon (2002), Structural analysis of the footwall fault block of the Moresby detachment (Woodlark rift basin) from borehole images, in *Proceedings of the Ocean Drilling Program, Scientific Results*, vol. 180, edited by B. Taylor, P. Huchon, and A. Klaus, pp. 1–43, Ocean Drilling Program, College Station, Texas, doi:10.2973/odp.proc.sr.180.165.2002.

McKenzie, D. P. (1969), The relation between fault plane solutions for earthquakes and the directions of the principal stresses, *Bulletin of the Seismological Society of America*, *59*(2), 591–601.

Orife, T., L. Arlegui, and R. J. Lisle (2002), Dipslip: a quickbasic stress inversion program for analysing sets of faults without slip lineations, *Computers & Geosciences*, *28*(6), 775 – 781, doi:DOI:10.1016/S0098-3004(01)00099-1.

Plateaux, R., N. Béthoux, F. Bergerat, and B. Mercier de Lépinay (2014), Volcano-

tectonic interactions revealed by inversion of focal mechanisms: stress field insight around and beneath the Vatnajökull ice cap in Iceland, *Frontiers in Earth Science*, *2*, 1–21, doi:10.3389/feart.2014.00009.

Provost, A.-S., and H. Houston (2001), Orientation of the stress field surrounding the creeping section of the San Andreas fault: Evidence for a narrow mechanically weak fault zone, *Journal of Geophysical Research: Solid Earth*, *106*(B6), 11,373–11,386, doi: 10.1029/2001JB900007.

Provost, A.-S., and H. Houston (2003a), Stress orientations in northern and central California: Evidence for the evolution of frictional strength along the San Andreas plate boundary system, *Journal of Geophysical Research: Solid Earth*, *108*(B3), doi: 10.1029/2001JB001123.

Provost, A.-S., and H. Houston (2003b), Investigation of temporal variations in stress orientations before and after four major earthquakes in California, *Physics of the Earth and Planetary Interiors*, *139*(3), 255 – 267, doi:10.1016/j.pepi.2003.09.007.

Reasenberg, P. A., and D. Oppenheimer (1985), *FPFIT, FPPLOT, and FPPAGE: Fortran computer programs for calculating and displaying earthquake fault-plane solutions*, *Open-File Report*, vol. 85-739, 109 pp., U.S. Geological Survey.

Rigo, A., P. Vernant, K. L. Feigl, X. Goula, G. Khazaradze, J. Talaya, L. Morel, J. Nicolas, S. Baize, J. Chéry, and M. Sylvander (2015), Present-day deformation of the Pyrenees revealed by GPS surveying and earthquake focal mechanisms until 2011, *Geophysical Journal International*, *201*(2), 947–964, doi:10.1093/gji/ggv052.

Tajima, F., and B. Célérier (1989), Possible focal mechanism change during reactivation of a previously ruptured subduction zone, *Geophysical Journal International*, *98*(2), 301–316, doi:10.1111/j.1365-246X.1989.tb03354.x.

Titus, S., H. Fossen, R. Pedersen, J. Vigneresse, and B. Tikoff (2002), Pull-apart formation and strike-slip partitioning in an obliquely divergent setting, Leka ophiolite, Norway, *Tectonophysics*, *354*(1), 101 – 119, doi:10.1016/S0040-1951(02)00293-7.

Yang, W., E. Hauksson, and P. M. Shearer (2012), Computing a large refined catalog of focal mechanisms for southern California (1981–2010): Temporal stability of the style of faulting, *Bulletin of the Seismological Society of America*, *102*(3), 1179–1194, doi:10.1785/0120110311.

Zeilinger, G., J. P. Burg, N. Chaudhry, H. Dawood, and S. Hussain (2000), Fault systems and Paleo-stress tensors in the Indus suture zone (NW Pakistan), *Journal of Asian Earth Sciences*, *18*(5), 547 – 559, doi:10.1016/S1367-9120(99)00084-X.